European Journal of Protistology 103 (2026) 126182

Contents lists available at ScienceDirect

European Journal of Protistology

journal homepage: www.elsevier.com/locate/ejop

Azadinium fusiforme, a new species of Amphidomataceae from Korean and Japanese coastal waters that lacks azaspiracid production

Urban Tillmann [a,*], Koyo Kuwata [b], Kyoungwon Cho [c], Kazuya Takahashi [b,d], Jan Tebben [a], Bernd Krock [a], Mitsunori Iwataki [b,*], Sunju Kim [c,*]

[a] Alfred Wegener Institut-Helmholtz Zentrum für Polar- und Meeresforschung, Ökologische Chemie, 27570 Bremerhaven, Germany
[b] Graduate School of Agricultural and Life Sciences, University of Tokyo, Tokyo 113-8657, Japan
[c] Major of Oceanography, Division of Earth Environmental System Science, Pukyong National University, Busan 48513, Republic of Korea
[d] Institute of Parasitology, Biology Centre, Czech Academy of Sciences, České Budějovice 370 05, Czech Republic

ARTICLE INFO

Keywords:
Azaspiracids
Amphidomataceae
Asia–Pacific region
Biogeography
Diversity
New species

ABSTRACT

The dinophyte family Amphidomataceae, comprising the genera *Azadinium* and *Amphidoma*, includes several species known to produce azaspiracids (AZAs), a group of lipophilic marine biotoxins associated with shellfish poisoning. Despite their ecological relevance and the increasing number of newly described species in recent years, their diversity is likely still underestimated, and knowledge of their global distribution and biogeography remains limited. Based on detailed morphological and phylogenetic analyses of strains from Korea and Japan, we describe *Azadinium fusiforme* sp. nov., a taxon that corresponds to the phylogenetic position of a strain previously reported from Japan. Light and scanning electron microscopy revealed that *Az. fusiforme* possesses a unique combination of morphological traits that distinguish it from its congeners. Notably, the ventral pore is located on the left side of the first apical plate, the pyrenoid is consistently positioned in the posteriormost part of the cell, the nucleus is elongated and centrally located, and pronounced thickenings occur along the sutures between the lateral and dorsal apical plates. Molecular data place *Az. fusiforme* in a well-supported, distinct clade within *Azadinium*, clearly supporting its designation as a new species. Mass spectrometric analyses showed no evidence of AZA production in any of the *Az. fusiforme* strains. This study contributes to a more fundamental understanding of the species diversity, distribution, and potential toxicity of Amphidomataceae in the Asia–Pacific region.

1. Introduction

Harmful algal blooms (HAB) are a recurring and intensifying issue in the Pacific coastal waters of Korea and Japan (Sakamoto et al., 2021). These blooms pose serious threats to marine ecosystems, aquaculture industries, and coastal economies. In recent decades, the frequency and spatial extent of HAB events have increased, with several toxic or harmful dinoflagellates (Lundholm et al., 2009), such as *Alexandrium*, *Karenia*, and *Margalefidinium*, regularly causing ecological and economic damage (Sakamoto et al., 2021). While traditional HAB-forming species such as *Margalefidinium polykrikoides* (Margalef) F. Gómez, Richlen & D. M. Anderson, *Alexandrium* spp., and *Karenia* spp. have long been the focus of monitoring and bloom-mitigation efforts, growing attention is now being paid to small, less conspicuous dinophytes in the family Amphidomataceae, which comprises the genera *Azadinium* and *Amphidoma*.

The presence of *Azadinium* in Korean waters was first reported by Potvin et al. (2012), who isolated a strain provisionally identified as *Azadinium* cf. *poporum* from Shiwha Bay on the west coast. At the time of analysis, none of the azaspiracid (AZA) toxins known then were detected in the Korean *Az. poporum* Tillmann & Elbrächter strain (Potvin et al., 2012), consistent with previous observations for the strain *Az. poporum* UTH-C8 (Tillmann et al., 2011). Subsequently, with the availability of additional strains of *Az. poporum* from Chinese coastal waters, the Korean strain was shown to belong to ribotype B of this species (Gu et al., 2013). These strains were later found to produce the newly discovered AZA-36 (in the European *Az. poporum* strain UTH-C8) and AZA-37 in the Korean strain (Krock et al., 2012, 2015). Overall, Potvin et al. (2012) marked the first recognition of Amphidomataceae in the Pacific Ocean and underscored the need for further investigation into their diversity,

* Corresponding authors.
E-mail addresses: urban.tillmann@awi.de (U. Tillmann), iwataki@g.ecc.u-tokyo.ac.jp (M. Iwataki), sunkim@pknu.ac.kr (S. Kim).

https://doi.org/10.1016/j.ejop.2026.126182
Received 18 November 2025; Received in revised form 12 January 2026; Accepted 13 January 2026
Available online 26 January 2026

ecological relevance, and toxigenicity. However, the diversity of Amphidomataceae in Korean waters remains underexplored, with only a limited number of morphologically and genetically identified species reported to date.

In contrast, studies in Japanese waters have yielded a broader range of Amphidomataceae diversity through active isolation efforts and long-term coastal surveys. One new species each of *Azadinium* (*Az. anteroporum* Kuwata, Kazuya Takahashi, W.M. Lum & Iwataki) and *Amphidoma* (*Am. fulgens* Kuwata, Kazuya Takahashi, W.M. Lum, G. Benico & Iwataki) were recently described (Kuwata et al., 2023, 2024b). Moreover, multiple ribotypes (A–C) of *Az. poporum* have been identified from Mutsu Bay and other nearshore areas, along with records of other taxa such as *Az. trinitatum* Tillmann & Nézan and *Az. zhuanum* Z. Luo, Tillmann & H. Gu (Ozawa et al., 2021; Takahashi et al., 2021). A recent study based on 81 *Azadinium* strains from Japanese waters substantially advanced knowledge on amphidomatacean diversity in the region by adding Northwest Pacific records of *Azadinium caudatum* (Halldal) Nézan & Chomérat, *Az. cuneatum* Tillmann & Nézan, *Az. dexteroporum* Percopo & Zingone, and *Az. spinosum* Elbrächter & Tillmann, and by describing *Az. inconspicuum* Kuwata, W.M. Lum, Kazuya Takahashi & Iwataki as a new species (Kuwata et al., 2025). Among these strains, AZAs were detected in *Az. poporum* (AZA-2, -11, -35, -36, -40, -59) and *Az. spinosum* (novel AZA) (Kuwata et al., 2025; Ozawa et al., 2021, 2023, 2025). Moreover, in that study, one strain (HrAz563), provisionally designated as *Azadinium* sp. 1, was phylogenetically distinct from all described *Azadinium* species; however, the strain was lost before detailed morphological observation could be conducted, precluding a formal species description (Kuwata et al., 2025).

To improve knowledge of the diversity of Amphidomataceae in the Northwest Pacific region, we successfully isolated two strains from Korean waters that correspond to the phylogenetic characteristics of *Azadinium* sp. 1, previously isolated from Japan and reported by Kuwata et al. (2025), thereby enabling the formal description of this taxon. Morphological observations using light and scanning electron microscopy of the two Korean strains, supplemented by additional light microscopy observations of the Japanese strain of *Azadinium* sp. 1, revealed morphological features including a distinct thecal plate arrangement that does not correspond to any currently described species. Phylogenetic analyses based on SSU, ITS, and LSU rDNA sequences confirmed its placement within the genus *Azadinium* and support its recognition as a novel species. The identification of this taxon further expands the known diversity of Amphidomataceae.

2. Materials and methods

2.1. Strain isolation, growth, and sampling

The Japanese strain HrAz563 was isolated from Hiroshima Bay, Seto Inland Sea (34°16′N, 132°16′E) in November 2018 (Kuwata et al., 2025). The two Korean strains, MPL-Az1-01 and MPL-Az1-02, were isolated from surface seawater collected at Mijo Harbor (34°42′53″N, 128°03′06″E) and Mulgun Harbor (34°47′37″N, 128°03′14″E), respectively, in Namhae, Korea, on 18 April 2022. Surface seawater samples (20 L each) were collected using a plastic bucket, pre-filtered through a 20 μm mesh, and subsequently concentrated using a 5 μm nylon mesh. The concentrated material was transferred into 50 mL conical tubes. *Azadinium*-like cells, characterized following the description by Tillmann et al. (2009), were isolated from the concentrated samples using a capillary pipette under an inverted microscope (AxioVert.A1; Zeiss, Jena, Germany), and were established as clonal cultures. Cultures were incubated at 20 °C under an irradiance of 160 μmol m^{-2} s^{-1} with a 14:10 h of light:dark cycle, and were maintained by biweekly transfer into fresh f/2-Si medium (salinity 30; Guillard and Ryther, 1962).

For toxin analysis, strains were grown under the standard culture conditions described above. For each harvest, cell density was determined by settling Lugol's iodine-fixed samples and counting more than 400 cells under an inverted microscope to calculate toxin cell quotas. Dense cultures (ca. 99–134 × 10^3 cells mL^{-1}) were harvested by centrifugation (5810R; Eppendorf, Hamburg, Germany) at 3220 × *g* for 10 min from 50 mL subsamples. The resulting cell pellets were resuspended, transferred into 2 mL microtubes, centrifuged again (5415; Eppendorf, Hamburg, Germany) at 16,000 × *g* for 5 min, and stored at −20 °C until analysis. Growth and harvest were replicated for strain MPL-Az1-01 to obtain high biomass (7–15 × 10^6 cells per replicate; $n = 3$). For strain MPL-Az1-02, one pellet of 14 × 10^6 cells was collected.

Genomic DNA was extracted using the Chelex extraction method described by Kim and Park (2014). Briefly, 2 mL of exponentially growing *Azadinium* culture was harvested by centrifugation at 13,500 × *g* for 5 min, and the supernatant was discarded. The cell pellet was transferred to a PCR tube and resuspended in 50 μL of 10% Chelex-100 solution (Bio-Rad, Hercules, CA, USA). Samples were heated at 95 °C for 1 h and centrifuged at 2860 × *g* for 5 min. The supernatant containing genomic DNA was transferred to a new PCR tube and stored at −20 °C until further analysis.

2.2. Microscopical analyses

Light microscopy (LM) observations of cells of strain MPL-Az1-01 were conducted using an inverted microscope (Axiovert 200 M; Zeiss, Jena, Germany) or a compound microscope (Axioskop 2; Zeiss), both equipped with differential interference contrast and epifluorescence optics. The shape and location of the nucleus were determined after staining of formalin-fixed cells with 4′,6-diamidino-2-phenylindole (DAPI; final concentration 0.1 μg mL^{-1}) for 10 min. Thecal tabulation was observed under an epifluorescence microscope (Axioskop 2; Zeiss) using UV excitation after staining with calcofluor white. Cell length and width were measured at 1000× magnification using Zeiss Axiovision software (Zeiss) based on photomicrographs of formaldehyde-fixed cells (1% final concentration). Photographs were acquired using an Axiocam MRc5 digital camera (Zeiss).

For scanning electron microscopy (SEM), cells were collected from 15 mL cultures by centrifugation (5810R, Eppendorf; 3220 × *g* for 10 min). After removal of the supernatant, the pellet was resuspended in 60% ethanol prepared in a 2-mL microtube with seawater (final salinity ca. 13) and incubated at 4 °C for 1 h to remove the outer cell membrane. Cells were then centrifuged again (5415R, Eppendorf) at 16,000 × *g* for 5 min, resuspended and fixed in a 60:40 mixture of deionized water and seawater (final salinity ca. 13) with 1% formaldehyde (final concentration), and stored at 4 °C for 3 h. Cells were collected on polycarbonate filters (25 mm across, 3 μm pore size; Millipore Merck, Darmstadt, Germany) using a filter funnel, in which all subsequent washing and dehydration steps were carried out. Filters were washed eight times with deionized water (2 mL each) and dehydrated through a graded ethanol series (30, 50, 70, 80, 95, and 100%; 10 min each). Final dehydration was performed using hexamethyldisilazane (HMDS), first in a 1:1 HMDS:ethanol mixture and then twice in 100% HMDS. Filters were air-dried in a desiccator under gentle vacuum. Finally, filters were mounted on stubs, sputter-coated with gold-palladium (SC500; Emscope, Ashford, UK), and examined at 10 kV using a FEG Quanta 200 SEM (FEI, Eindhoven, The Netherlands). Micrographs were processed on a black background using Photoshop 6.0 (Adobe Systems, San Jose, CA, USA). The Kofoidean plate tabulation nomenclature was used for plate labeling.

2.3. Sequencing and phylogenetic analyses

PCR amplification was performed using the following primer pairs: EUKA (5′-AAC CTG GTT GAT CCT GCC AGT-3′) and EUKB (5′-AKA TGC TTA ART TCA GCR GG-3′) for the SSU rRNA gene (Medlin et al., 1988); 1662F (5′-CCG ATT GAG TGW TCC GGT GAA TAA-3′) and 25R1 (5′-CTT GGT CCG TGT TTC AAG AC-3′) for the internal transcribed spacer (ITS1, 5.8S rRNA, ITS2) region (Handy et al., 2009), and D1R (5′-ACC CGC TGA

ATT TAA GCA TA-3′) and 1483R (5′-GCT ACT ACC ACC AAG ATC TGC-3′) for the LSU rRNA gene (Daugbjerg et al., 2000; Nunn et al., 1996). PCR reactions were conducted in a total volume of 20 μL, containing 2 μL of template DNA, forward and reverse primers each at a final concentration of 0.3 μM, and deionized sterile water, using an AccuPower PCR premix (Bioneer, Daejeon, Korea). Amplifications were performed on a C1000 Touch thermal cycler (Bio-Rad, Hercules, CA, USA) under the following conditions: initial denaturation at 94 °C for 2 min, 35 cycles of denaturation at 94 °C for 30 s, annealing at 52–55 °C for 30–45 s, and extension at 72 °C for 1–2 min; followed by a final extension at 72 °C for 7 min. PCR products were visualized on 1% agarose gels stained with EcoDye (SolGent Co., Daejeon, Korea), and purified using ExoSAP-IT™ (Thermo Fisher Scientific, Wilmington, DE, USA). Sequencing was performed with the corresponding primers using a Big-Dye Terminator v3.1 Cycle Sequencing kit (Applied Biosystems, Foster City, CA, USA) on an ABI PRISM 3730xl Analyzer (Applied Biosystems). Sequence reads were assembled, and low-quality regions were manually edited using ContigExpress (Vector NTI ver. 10.1; Invitrogen, Grand Island, NY, USA). The assembled sequences were verified by BLASTN searches against the NCBI database and deposited in GenBank (accession numbers PV915287 and PV915288).

A total of 98 sequences (SSU rDNA, ITS1, 5.8S rDNA, ITS2, and LSU rDNA) from *Azadinium* and *Amphidoma* species, including three strains of *Az. fusiforme* sp. nov. (MPL-Az1-01, MPL-Az1-02, HrAz563), were retrieved from GenBank (Supplementary information S1, Table S1), and aligned using MAFFT ver. 7.10 (Katoh et al., 2019). Ambiguously aligned sites were excluded using MEGA11 (Tamura et al., 2021), yielding a final alignment of 4176 bp. The best-fitting substitution model was selected using jModelTest (Posada, 2008) under the Akaike information criterion (AIC). Bayesian inference (BI) was conducted using MrBayes ver. 3.2 (Ronquist et al., 2012) with the GTR + G + I model. Four Markov chain Monte Carlo (MCMC) chains were run for 10,000,000 generations, sampling every 1000 generations. Convergence was assessed using Tracer ver. 1.7 (Rambaut et al., 2018), and the first 10% of the samples were discarded as burn-in, well after stationarity had been reached. Posterior probabilities were calculated from a majority-rule consensus tree. Maximum likelihood (ML) analysis was performed using IQ-TREE 3 (Minh et al., 2020; Wong et al., 2025) under the same substitution model, with branch support estimated from 2000 ultrafast bootstrap (UFB) replicates.

2.4. AZA analysis

2.4.1. Extraction

Aqueous pellets containing 7–15 × 10^6 cells were dried under a gentle stream of nitrogen, and the residues were extracted with 200 μL of acetone for 1 h. Subsequently, the pellets were repeatedly resuspended by pipetting and vortexing (Vortex 560E, Scientific Industries). The homogenates were then centrifuged at 21,130 × *g* (model 5424 R, Eppendorf). The supernatants were transferred to HPLC vials and stored at −20 °C until analysis.

2.4.2. Mass spectrometric analysis

The initial mass spectrometric screening of extracts from strains MPL-Az1-01 and MPL-Az1-02 showed no evidence of the presence of known AZAs. To verify the absence of known AZAs or structural analogues producing characteristic AZA fragment ions, high biomass extracts (see Section 2.1) were further analyzed using an Agilent 1100 liquid chromatograph (LC) (Agilent, Waldbronn, Germany) coupled to a triple quadrupole mass spectrometer (4000 QTRAP; Sciex, Darmstadt, Germany), as well as a Vanquish UHPLC coupled to a high-resolution Orbitrap Exploris 480 mass spectrometer (Thermo Scientific, Bremen, Germany). Detailed conditions for liquid chromatography and mass spectrometric analyses, including selected reaction monitoring (SRM), untargeted analysis by precursor ion scan (PREC) and untargeted high-resolution data independent analysis (DIA), are provided in Supplementary information S2 (Tables S2 and S3; Figs. S1–S4).

3. Results

Three strains from two geographic regions, the Korean and Japanese coastal waters, were available for analysis. All strains exhibited identical characters, as far as could be observed. The holotype material was prepared from one of the Korean strains (MPL-Az1-01), which served as the basis for the detailed morphological description presented below (Figs. 1–5). The Japanese strain HrAz563, provisionally referred to as *Azadinium* sp. 1 and illustrated by two light micrographs in Kuwata et al. (2025), is documented here in greater detail in the Supplementary Information, including an additional plate of photomicrographs and calcofluor-stained cells examined under epifluorescence microscopy (Supplementary Information S3, Fig. S5).

3.1. Description of *Azadinium fusiforme* Kuwata, Tillmann, Sunju Kim, Kazuya Takahashi et Iwataki sp. nov.

Description. Marine, phototrophic, thecate dinoflagellate. Cells fusiform to biconical, measuring 13.9–21.0 μm in length and 8.9–14.0 μm in width. Episome roundly conical with a prominent apical pore complex. Hyposome shorter than the episome and broader than high. Cingulum approximately one-sixth of the total cell length. Thecal plate formula: po, cp, X, 4', 3a, 6", 6C, 5S, 6‴, 2⁗. Ventral pore located on the left side of the first apical plate; a single antapical spine located posteriorly on the right side of the cell. The nucleus elongated and centrally positioned. A brownish chloroplast located peripherally; a spherical pyrenoid situated in the posterior region of the cell.

Holotype. SEM stub prepared from clonal strain MPL-Az1-01 (designated CEDiTH206), deposited in the Senckenberg Research Institute and Natural History Museum, Centre of Excellence for Dinophyte Taxonomy (Wilhelmshaven, Germany), and used for the observations shown in Figs. 2–4.

Reference material. Formalin-fixed sample prepared from clonal strain MPL-Az1-01 (designated CEDiTRM207) deposited at the Senckenberg Research Institute and Natural History Museum, Centre of Excellence for Dinophyte Taxonomy (Wilhelmshaven, Germany).

Type locality. Mijo Harbor, Namhae, Republic of Korea.

Habitat. Marine plankton.

Strain establishment. Sampled and isolated by S. Kim.

Etymology. The specific epithet *fusiforme* (Latin, derived from *fusus* = spindle, and *forma* = shape) refers to the characteristic spindle-shaped morphology of the species.

Registration. This taxonomic act has been registered in PhycoBank (ID: 106468). SSU rDNA, ITS, and LSU rDNA sequences have been registered in GenBank (accession number PV915288; MPL-Az1-01).

At low magnification, cells of *Azadinium fusiforme* revealed the characteristic swimming behavior typical of the genus *Azadinium* (Supplementary Video). Cells generally moved relatively slowly, with occasional short, abrupt jumps in various directions. These jumps were most frequently observed when cells approached the bottom of the observation chamber. In rare instances, cells traversed longer distances at higher speeds.

Cells of *Az. fusiforme* were fusiform to biconical in shape (Fig. 1), with a length-to-width (L/W) ratio ranging from approximately 1.46 to 1.78, and exhibited moderate size variability. The Korean strain MPL-Az1-01 had a mean length of 16.9 ± 1.4 μm (range: 13.9–19.9 μm; n = 55) and a mean width of 10.7 ± 0.8 μm (range: 8.9–12.9 μm; n = 55). By comparison, the Japanese strain HrAz563 measured 18.8 ± 1.4 μm in length (range: 16.4–21.1 μm; n = 22) and 12.3 ± 1.3 μm in width (range: 9.5–14.3 μm; n = 22). Both the episome and hyposome were broadly conical, with the episome being larger and wider than the hyposome (Fig. 1A–I), and terminating in a distinct, rounded apical pore complex (APC) (Fig. 1A, C). In lateral view, cells appeared only slightly compressed along the dorsoventral axis (Fig. 1G). The cingulum was situated

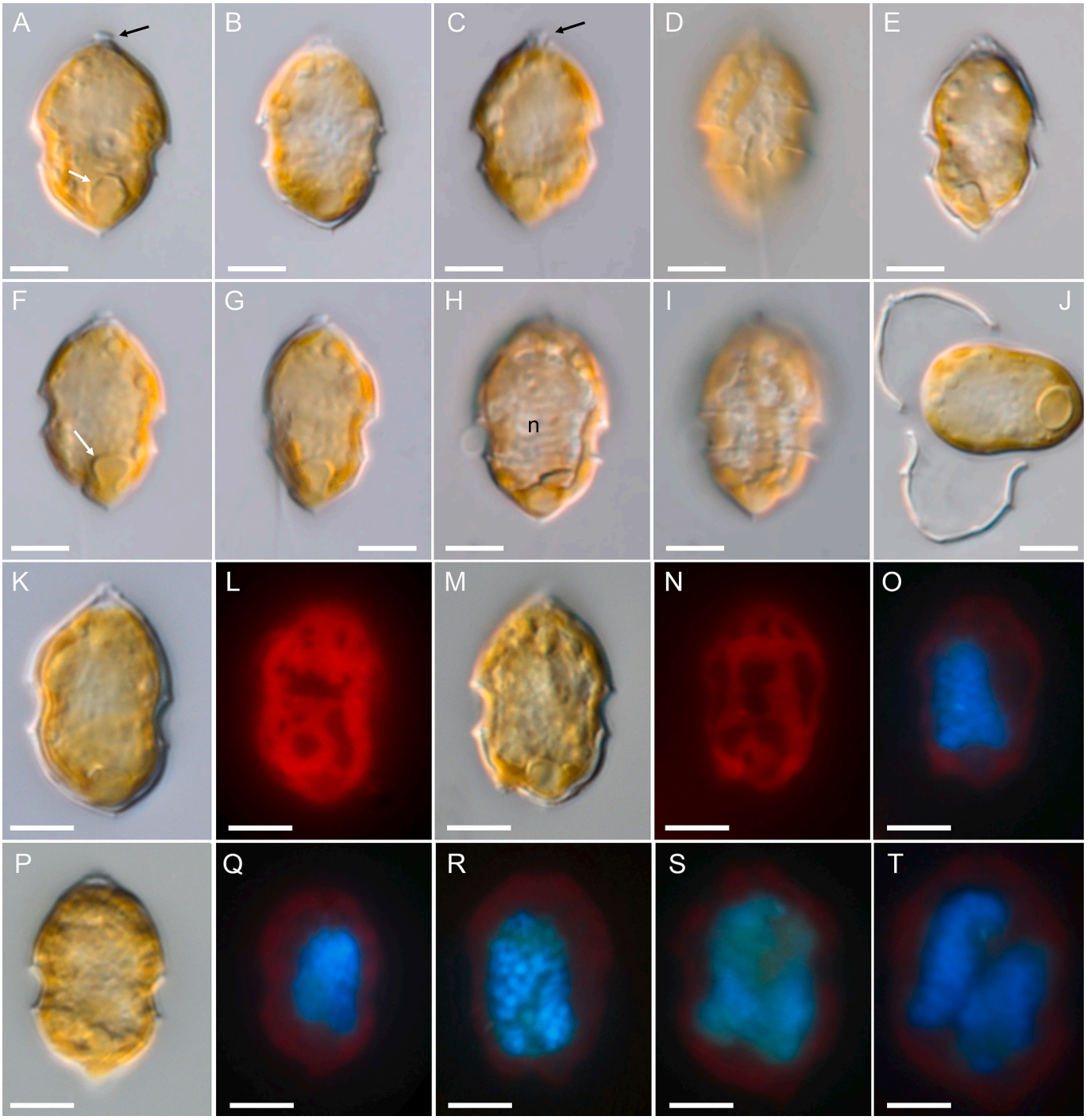

Fig. 1. *Azadinium fusiforme* sp. nov. (strain MPL-Az1-01). LM of live cells (A–J) or formalin-fixed cells (K–T). (**A–I**) General size and shape of cells in dorsal/ventral (A–E), ventral-lateral (F), and lateral (G–I) views. Note the prominent apical pore complex (black arrow in A and C), the pyrenoid (white arrow in A and F) in the hyposome, and elongated nucleus (n) with visible chromosomes (H), and the reticulate structure of the chloroplast (I). (**J**) A cell during ecdysis; the cell is emerging from the theca, with the epitheca detached ventrally from the cingulum and hypotheca. (**K**, **L**) The same cell in brightfield (K) and with blue light excitation (L) showing the reticulate chloroplast in red. (**M–O**) The same cell stained with DAPI and observed with brightfield (M), under blue light excitation (N) or with UV light excitation (O), indicating the shape, size and position of the chloroplast (red) and the nucleus (blue). (**P–T**) Other cells stained with DAPI with UV light excitation. Cells in early stage (R) or late stages (S, T) of cell division. Scale bars = 5 µm. (For interpretation of the references to colour in this figure legend, the reader is referred to the web version of this article.)

slightly below the equatorial plane and displaced by approximately one-third to one-half of its own width (Fig. 1D). A distinct antapical spine projected from a more or less pointed posterior end of the cell's right side (Fig. 1A, E–I). A single, large pyrenoid surrounded by a starch sheath was visible in the posterior hyposome (Fig. 1A, F). The brownish to orange chloroplast was positioned peripherally and exhibited a reticulate structure visible under light microscopy (Fig. 1D, I), and particularly pronounced under epifluorescence microscopy (Fig. 1K–N). Ecdysis was frequently observed, presumably triggered by stress during microscopic observation. During this process, the rounded protoplast emerged from the theca following loss of flagella, rendering thecal plates clearly discernible (Fig. 1J). The large, ellipsoidal nucleus was centrally

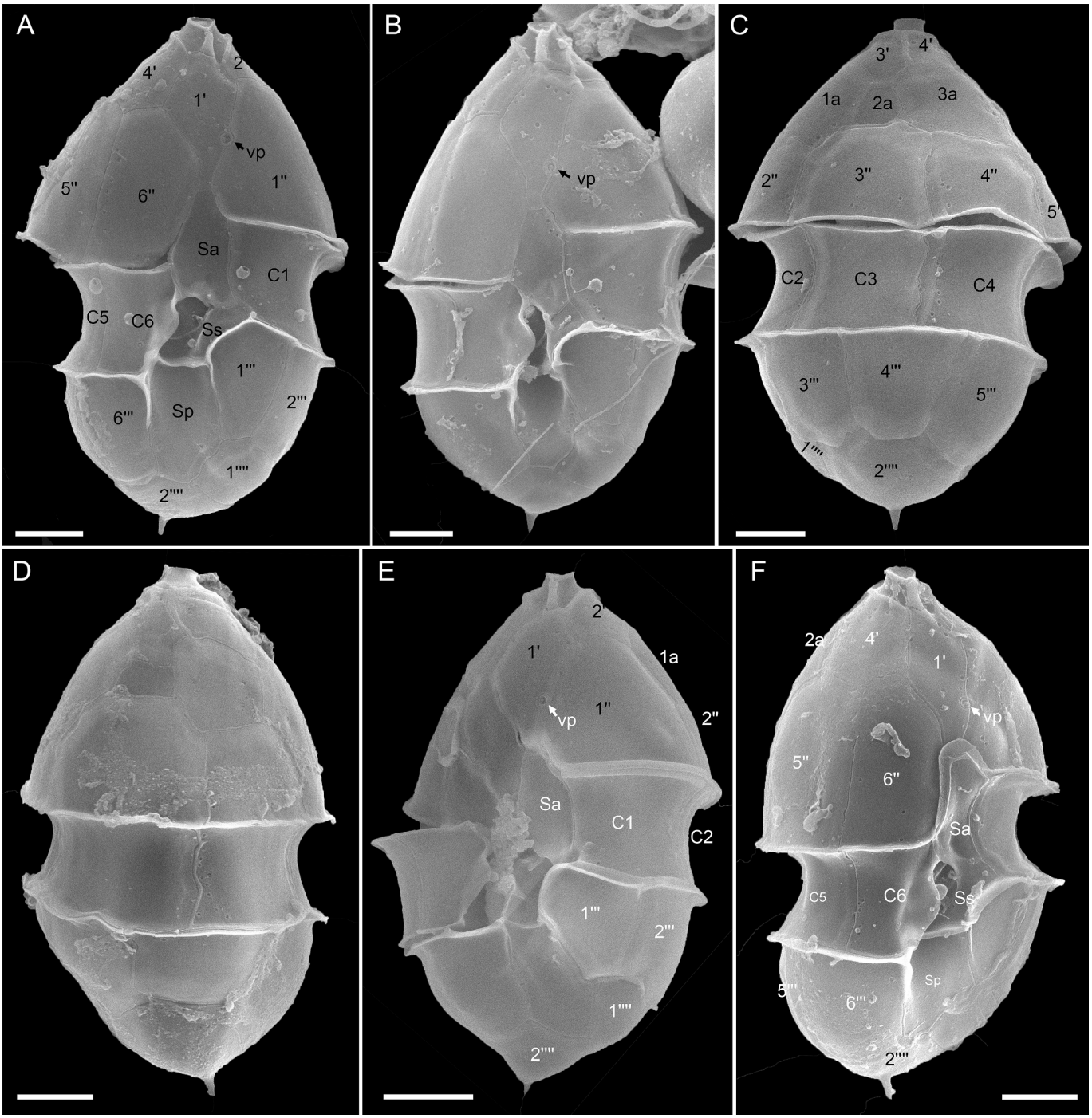

Fig. 2. *Azadinium fusiforme* sp. nov. (strain MPL-Az1-01). SEM micrographs of different cells in ventral (A, B), dorsal (C, D), ventral left-lateral (E), and ventral right-lateral (F) views. Note the location of the ventral pore (vp). Scale bars = 2 μm.

positioned and typically extended into the hyposome (Fig. 1H, O–T). During mitosis, the nucleus elongated and divided perpendicular to the longitudinal axis of the cell (Fig. 1R–T).

The delicate theca could be stained using calcofluor white (Fig. S5). However, due to the small cell size and fragile plates, detailed characterization of the thecal plate pattern in strain MPL-Az1-01 was accomplished by scanning electron microscopy (SEM) (Figs. 2–4). For strain HrAz563, only micrographs based on calcofluor staining were available (Fig. S5), as the strain was lost before SEM observations could be conducted. The plate formula was determined as po, cp, X, 4', 3a, 6", 6C, 5S, 6''', 2'''' (Figs. 2–4). SEM observations confirmed the slender fusiform cell shape (Fig. 2), the slight dorsoventral compression (Fig. 2F), the prominent antapical spine (Fig. 2A–F), the pointed apical pore bordered by a raised rim (Fig. 2A–F), and the displaced cingulum (Fig. 2A, B, E). A ventral pore was located on the left side of the first apical plate, approximately midway between its anterior and posterior margins (Fig. 2A, B, E). The ventral pore had a diameter of 0.41 ± 0.03 μm (range 0.36–0.48 μm; n = 20), including the distinct, platelet-like structure surrounding the central opening.

The epitheca (Fig. 3) consisted of 16 plates. The apical series comprised four plates. Plate 1' was ortho but asymmetrical, with its suture with plate 6" being shorter than that with plate 1" (Fig. 3A). Among the lateral apical plates, plate 2' was pentagonal and distinctly smaller than the hexagonal plate 4' (Fig. 3A, C–E). The dorsal apical

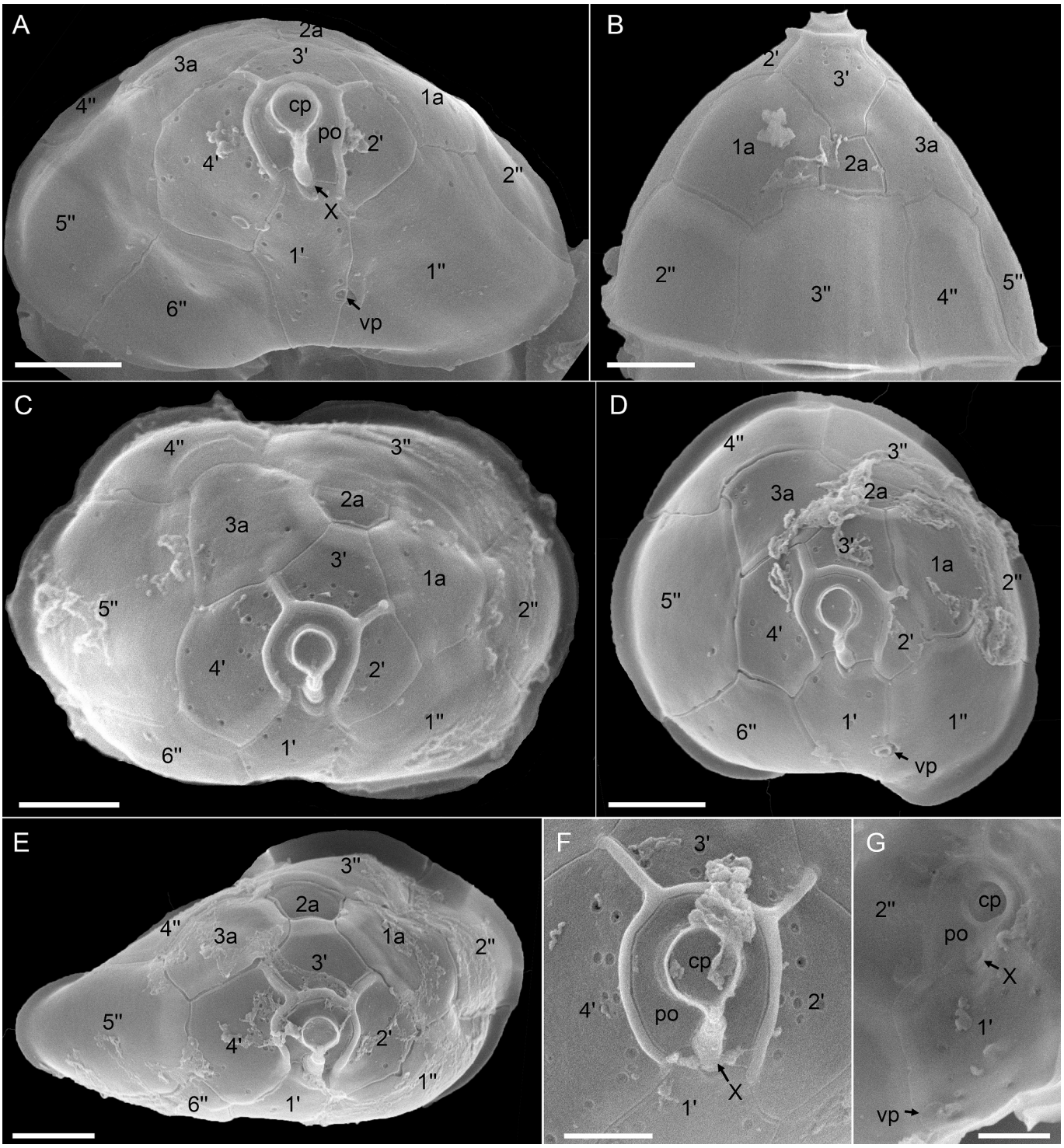

Fig. 3. *Azadinium fusiforme* sp. nov. (strain MPL-Az1-01). SEM micrographs of different thecae. (**A–E**) Epithecal plates in ventral (A), dorsal (B), and apical (C–E) views. (**F, G**) Details of the apical pore complex in external (F) and internal (G) views. cp, cover plate; po, pore plate; X, X-plate; 1'–6', apical plates; 1"–6", precingular plates; vp, ventral pore. Scale bars = 1 μm (F, G) and 2 μm (A–E).

plate 3' was hexagonal, broad anteriorly and narrow posteriorly (Fig. 3B–E). The apical pore (Fig. 3A–G) was round to slightly ellipsoidal, overlaid by a cover plate (cp) and centered on a slightly elongated pore plate (po), which was bluntly truncated dorsally at the junction with plate 1'. A small X-plate (canal plate) was located where the pore plate contacted plate 1', best observed in internal view (Fig. 3G). Externally, the X-plate displayed a characteristic three-dimensional morphology, including a finger-like projection connected to the apical cover plate (Fig. 3F). A prominent raised rim surrounded the pore plate, formed by adjacent apical plates 2', 3', and 4'. Notably, this rim extended dorsally along the sutures between the lateral apical plates and plate 3' (Fig. 3A, C–F). The three anterior intercalary plates were arranged more or less symmetrically on the dorsal side of the epitheca (Fig. 3B–E). Plates 1a and 3a were hexagonal and similar in size and larger than the four-sided plate 2a, which was positioned above precingular plate 3" (Fig. 3B–E). The six precingular plates were of

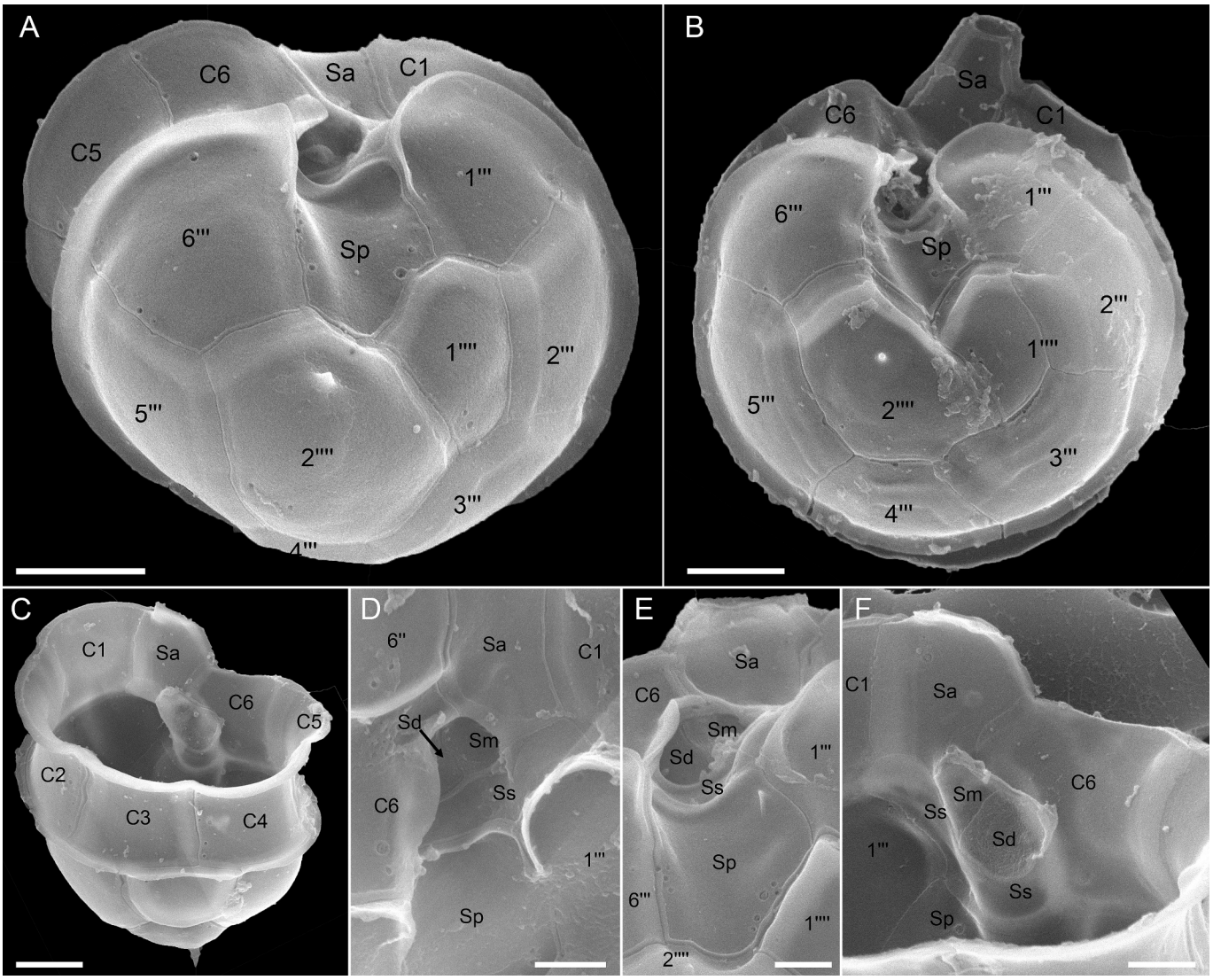

Fig. 4. *Azadinium fusiforme* sp. nov. (strain MPL-Az1-01). SEM micrographs of different thecae. (**A, B**) Hypothecal plates in antapical view. (**C**) Hypotheca in dorso-apical view to illustrate the cingular plates. (**D–F**) Details of sulcal plates in external (D, E) and internal (F) views. C1–C6, cingular plates; Sa, anterior sulcal plate; Sd, right sulcal plate; Sm, median sulcal plate; Sp, posterior sulcal plate; Ss, left sulcal plate; 1'''–6''', postcingular plates; 1'''' and 2'''', antapical plates. Scale bars = 1 μm (D–F) and 2 μm (A–C).

comparable width and height. Plate 1" was hexagonal with a broad suture with intercalary plate 1a, whereas plate 6" was pentagonal and did not contact any anterior intercalary plate.

The hypotheca comprised six postcingular and two antapical plates (Fig. 4). Among the postcingular plates, plate 3''' was rectangular and contacted both antapical plates, while the other plates of this series were also rectangular, with plate 5''' being slightly larger (Fig. 4A, B). The two antapical plates were unequal in size, with the hexagonal plate 2'''' approximately twice as large as the pentagonal plate 1'''' (Fig. 4A, B). Plate 2'''' bore the antapical spine, which was positioned closer to the posterior sulcal plate (Sp) than to the dorsal postcingular plate 4''' (Fig. 4A, B). The broad and incised cingulum consisted of six cingular plates (Fig. 4C) that were generally similar in size, although plate C2 plate was slightly broader and plate C6 slightly narrower. All cingular plate sutures were nearly aligned with the respective sutures of precingular plates (Fig. 2). In the deeply concave sulcus, five sulcal plates were identified (Fig. 4D–F). A large, anterior sulcal plate (Sa), tapering anteriorly, extended partially into the epitheca. The large posterior sulcal plate (Sp) was pentagonal and extended about two-thirds of hypotheca's length from the cingulum to the antapex. The left sulcal plate (Ss), located anterior to Sp, abutted both terminal cingular plates (C1 and C6) and was of roughly uniform width. The central sulcal area around the flagellar pore was internally vaulted and composed of plates Sm and Sd, which were best visualized in internal view (Fig. 4F).

The thecal plates were smooth and irregularly perforated by small pores (Figs. 2–4). The highest pore densities were observed on the epitheca (Fig. 3A–F), particularly on the apical and lateral intercalary plates, which bore up to approximately 10 pores per plate. In contrast, the precingular plates each bore only a few pores, and the central intercalary plate consistently lacked pores. On the hypotheca, only isolated pores or small clusters (up to four per plate) were present, while the central sulcal plates Sm and Sd were free of pores (Fig. 4). The cingular plates occasionally exhibited short vertical rows of pores along the sutures (Fig. 4C). Pore diameters averaged approximately 0.1 μm but were highly variable, ranging from 0.06 to 0.18 μm. It remains uncertain whether the smallest structures observed actually represent true thecal pores penetrating the plate surface.

The plate tabulation and arrangement illustrated in Figure 5 represents the most common configuration observed in *Az. fusiforme* cultures. However, several deviations were observed in cultured material (Figs.

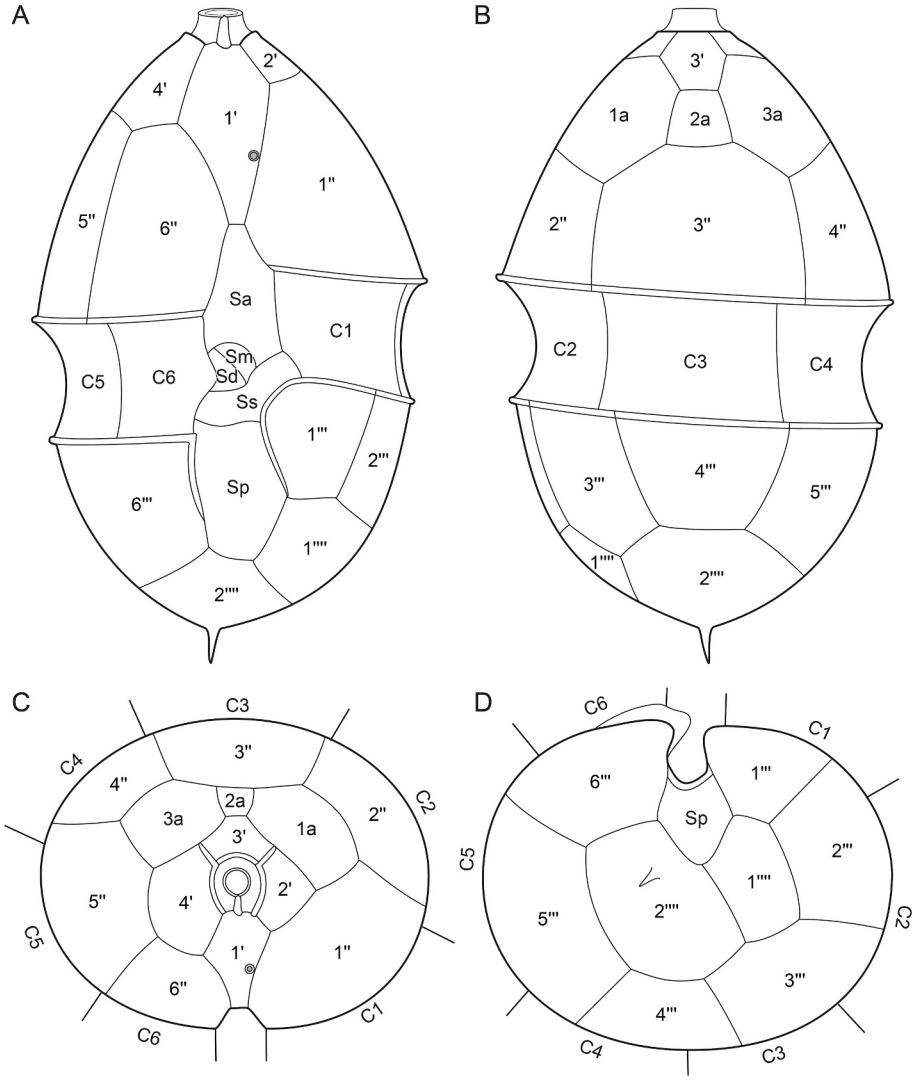

Fig. 5. *Azadinium fusiforme*. Diagrammatic illustration of thecal plate configurations. (**A**) Ventral view. (**B**) Dorsal view. (**C**) Apical view. (**D**) Antapical view.

S6, S7). The small central anterior intercalary plate 2a was normally tetragonal and contacted a single precingular plate, but in one specimen it was symmetrical and pentagonal, contacting two precingular plates (Fig. S6A). Additional plates were most frequently observed on the epitheca, typically arising from division of plate 2a (Fig. S6B, C) or from division of apical plates or dorsal precingular plates (Fig. S6E–M). Very rarely, a reduction in the number of epithecal plates was observed, for example through the absence of the suture between plates Sa and 1' (Fig. S6D). The antapical spine, which was readily visible in most specimens even under light microscopy, varied in length and was occasionally reduced to a small knob (Fig. S7B, C). In rare cases, no antapical spine was detected (Fig. S7D, E), and one specimen exhibited two spines (Fig. S7A). In the hypotheca, a reduction in the number of postcingular plates to five was observed (Fig. S7F, G). Minor variation was also observed in the development of the raised rim along apical plate sutures. In rare cases, the rim along individual sutures was only rudimentarily developed (Fig. S7H, K), or almost completely absent, sometimes accompanied by irregularities in the rim surrounding the pore plate (Fig. S7J, K).

3.2. Azaspiracid analyses

Analyses with a triple quadrupole mass spectrometer using selected reaction monitoring (SRM) for known AZAs (Table S2) and untargeted precursor ion scan (PREC) for characteristic AZA daughter ions (e.g., *m/z* 348, *m/z* 350, *m/z* 360, *m/z* 362, and *m/z* 378), showed no evidence of AZA production (limits of detection [LoDs] are given in Table S3). In addition, untargeted high-resolution data-independent analysis (DIA) was employed to screen for azaspiracids (AZAs) by systematically fragmenting defined *m/z* windows and subsequently searching for daughter-ion masses corresponding to common AZA fragments (± 10 ppm; Table S2). Using this approach, the major fragments of AZA-1 (i.e., *m/z* 154, 362, 462) were readily detected following the injection of an AZA-1 standard (Figs. S1, S2) or an extract equivalent to ~900 cells (on-column) of *Az. spinosum* (Fig. S3; cell quota: 140 fg cell^{-1}). In contrast, injection of extracts equivalent to up to 377,000 cells on-column from *Az. fusiforme* (MPL-Az1-01; $n = 3$) did not yield any identifiable AZA peaks (Fig. S3; calculated LoD = 0.35 fg μL^{-1}) when compared with known AZA fragment ions.

3.3. Molecular phylogeny

Pairwise comparisons among the three *Az. fusiforme* strains (MPL-Az1-01, MPL-Az1-02, and HrAz563) revealed identical LSU rRNA gene sequences. In contrast, comparison of the Korean strain (MPL-Az1-01)

with the Japanese strain (HrAz563) identified four base-pair differences in the ITS1–5.8S rRNA gene–ITS2 region sequences (670 bp in length), corresponding to 99.4% similarity. The SSU rRNA gene sequence was obtained only from the Korean strain (MPL-Az1-01).

Maximum likelihood (ML) and Bayesian inference (BI) analyses based on concatenated SSU rRNA, ITS region, and LSU rRNA gene sequences produced largely congruent tree topologies, differing only in the placement of *Az. caudatum* var. *caudatum*, *Az. caudatum* var. *margalefii*, and *Az. galwayense* R. Salas & Tillmann (Fig. 6). Both analyses supported a monophyletic clade comprising all *Azadinium* species (BI/UFB = 1.00/100%). In the BI tree (Fig. 6), ribotypes of *Az. poporum* formed a monophyletic clade and were closely related to sequences of *Az. dalianense* Z. Luo, H. Gu & Tillmann, although this relationship received only moderate support (0.83/72%). Sequences of *Az. fusiforme* branched as a sister lineage to the *Az. poporum* and *Az. dalianense* group, but this relationship was weakly supported (<0.70/80%).

Fig. 6. Molecular phylogeny of *Azadinium* and *Amphidoma* inferred from concatenated SSU, ITS–5.8S region, and LSU rRNA gene sequences using Bayesian inference (BI). Sequences of *Az. fusiforme* are highlighted in red. Numbers above branches indicate statistical support values (left: Bayesian posterior probabilities, BPP; right: ultrafast bootstrap support values, UFB). Only BPP ≥ 0.7 and UFB ≥ 80% are shown. Asterisks (*) denote maximal support (BPP = 1.00; UFB = 100%). (For interpretation of the references to colour in this figure legend, the reader is referred to the web version of this article.)

4. Discussion

The integration of detailed morphological examinations and molecular phylogenetic analyses provides compelling evidence for the recognition of *Azadinium fusiforme* sp. nov. as a distinct species within the genus *Azadinium*. The newly isolated Korean strains, along with the Japanese strain HrAz563, provisionally identified as *Azadinium* sp. 1 by Kuwata et al. (2025), consistently exhibit the diagnostic plate tabulation characteristic of the genus, including four apical plates, three anterior intercalary plates, and six plates each in the precingular and postcingular series, as well as two antapical plates (Tillmann et al., 2009).

This morphological conformity, together with the molecular data, which place *Az. fusiforme* in a separate and well-supported clade within *Azadinium*, clearly supports its delineation as a new species. While *Az. fusiforme* shares general morphological similarities—such as cell size and shape—with other congeners, it exhibits a unique combination of distinguishing features, visible both under light microscopy and scanning electron microscopy. These unique traits, in combination with phylogenetic distinctiveness, justify the formal description of *Azadinium fusiforme* sp. nov. and confirm its systematic placement within the Amphidomataceae.

Previous investigations into the genus *Azadinium* have emphasized the diagnostic relevance of ventral pore (vp) position for distinguishing between species (Kuwata et al., 2023; Salas et al., 2021; Tillmann et al., 2011). In amphidomatacean taxa, the vp is significantly larger than standard thecal pores, surrounded by a distinct, plate-like structure, and its location on the ventral surface of the epitheca varies in a species-specific manner (Tillmann and Akselman, 2016; Tillmann et al., 2012a). In *Az. fusiforme*, the vp is located ventrally on the left side of the first apical plate. This configuration sets the species apart from all other known *Azadinium* taxa in which the vp is either in direct contact with, or even situated within, the pore plate, being either positioned centrally as in *Az. anteroporum* (Kuwata et al., 2023), left of the longitudinal axis in *Az. poporum*, *Az. dalianense*, *Az. cuneatum*, and *Az. trinitatum* (Luo et al., 2013; Tillmann et al., 2011, 2014), or right of it in *Az. caudatum* var. *margalefii*, *Az. dexteroporum*, *Az. concinnum* Tillmann & Nézan, *Az. luciferelloides* Tillmann & Akselman, *Az. zhuanum*, *Az. perforatum* Tillmann, Wietkamp & H. Gu, *Az. galwayense*, *Az. perfusorium* Tillmann & R. Salas, and *Az. inconspicuum* (Kuwata et al., 2025; Luo et al., 2017; Nézan et al., 2012; Percopo et al., 2013; Salas et al., 2021; Tillmann and Akselman, 2016; Tillmann et al., 2014, 2020). Another taxon lacking vp contact with the pore plate is *Az. caudatum* var. *caudatum* (Nézan et al., 2012); however, in that case, the vp is positioned on the right side of the first apical plate and is thus clearly distinct from the left-sided vp of *Az. fusiforme*.

As a result, a more detailed comparison is warranted with those species in which the ventral pore is likewise positioned on the left side of the first apical plate. These include *Az. spinosum*, *Az. obesum* Tillmann & Elbrächter, *Az. polongum* Tillmann, the provisionally named *Az.* cf. *spinosum*, and *Az. asperum* Tillmann (Table 1).

Azadinium asperum has only been described based on SEM observations of fixed, archived material, and therefore, information on light microscopical features (such as the nucleus and pyrenoid) is not available (Tillmann, 2018). Nevertheless, the species is markedly larger and characterized by a slightly rough, granular thecal surface. In addition, the vp of *Az. fusiforme* is located near the suture to the first precingular plate (1"), whereas that of *Az. asperum* is located near the suture to the second apical plate (2'), which clearly distinguishes it from *Az. fusiforme*. *Azadinium polongum* shares the ventral pore position with *Az. fusiforme* and also possesses an antapical spine (Tillmann et al., 2012b). However, it is considerably less slender and differs from *Az. fusiforme* particularly by a distinctly elongated pore plate as well as a markedly extended X-plate. *Azadinium obesum* is clearly distinguishable from *Az. fusiforme* by its broader cell shape and the absence of both a pyrenoid and an antapical spine (Tillmann et al., 2010). In addition, unlike *Az. fusiforme*, *Az. obesum* shows no contact between plate 1a and plate 1".

The species most closely resembling *Az. fusiforme* is the type species of the genus, *Az. spinosum*. Although *Az. fusiforme* (mean 16.9 µm in length) is slightly larger than *Az. spinosum* (mean 13.8 µm in length), both species are similar in their slender, fusiform shape, the presence of an antapical spine, and the general position of the ventral pore, as well as in the size and arrangement of all thecal plates (Tillmann et al., 2009). However, notable differences are apparent under light microscopy. In *Az. spinosum*, the pyrenoid—clearly visible due to its surrounding starch sheath—is consistently located in the episome. In contrast, the pyrenoid in *Az. fusiforme* is always positioned in the posteriormost part of the cell. Furthermore, nuclear shape and position differ; in *Az. spinosum*, the nucleus is generally more spherical to ovoid and situated in the lower third of the cell, whereas in *Az. fusiforme*, the nucleus tends to be more elongated and centrally located. It should be noted that in *Azadinium*, nuclear morphology is known to vary during the cell cycle (Tillmann and Elbrächter, 2013). However, the elongated nucleus in *Az. fusiforme* is consistently observed and not limited to dividing cells. Despite the overall similarity between *Az. fusiforme* and *Az. spinosum* in electron microscopy, one notable ultrastructural difference exists: in *Az. fusiforme*, the sutures of the lateral and dorsal apical plates are thickened by a prominent rim, a feature that is absent in *Az. spinosum*.

The comparison of *Az. fusiforme* with other taxa that share a similar ventral pore position also includes the taxon currently and provisionally referred to as *Azadinium* cf. *spinosum*. A formal species description has not yet been established for this taxon. While *Az.* cf. *spinosum* is phylogenetically distinct and well supported as being positioned outside the *Az. spinosum* clade in rDNA sequence-based trees, it cannot be distinguished morphologically—neither under light microscopy nor SEM—from *Az. spinosum* (Tillmann et al., 2021). Consequently, *Az. fusiforme* can be differentiated from *Az.* cf. *spinosum* based on the same set of morphological and ultrastructural characters used to separate it from *Az. spinosum*.

Table 1
Compilation of morphological features of *Azadinium* species (including the new species *Az. fusiforme*) with a ventral pore located on the left side of the first apical plate.

	Az. fusiforme	*Az. spinosum*	*Az. obesum*	*Az. polongum*	*Az.* cf. *spinosum*	*Az. asperum*
Cell length (µm)	13.9–21.0	12.3–15.7	13.3–17.7	10.1–17.4	13.4–18.7	21.1–26.0
Cell width (µm)	8.9–14.0	7.4–10.3	10.0–14.3	7.4–13.6	8.1–12.9	17.4–21.6
Length/width ratio	1.6	1.6	1.3	1.3	1.6	1.2
Pyrenoid with starch sheath	one, posterior	one, episome	no	no	one, episome	n.a.
Nucleus	elongated, central	spherical, posterior	spherical, posterior	spherical, central	spherical, posterior	n.a.
Ventral pore	suture of 1' and 1"	suture of 1' and 1"	suture of 1' and 1"	suture of 1' and 1"	suture of 1' and 1"	suture of 1' and 2'
Pore plate (po)	round to ellipsoidal	round to ellipsoidal	round to ellipsoidal	elongated	round to ellipsoidal	ellipsoidal
X plate	round	round	round	elongated	round	round
1" in contact with 1a	yes	yes	no	yes	yes	yes/no
Rim along sutures of 2', 3' and 4'	yes	no	no	no	no	yes
Antapical spine	yes	yes	no	yes	yes	yes
Plate surface	smooth	smooth	smooth	smooth	smooth	rough
AZA production	no	yes	no	no	no	n.a.
Reference	This study	Tillmann et al. (2009)	Tillmann et al. (2010)	Tillmann et al. (2012b)	Tillmann et al. (2021)	Tillmann (2018)

Finally, the significance of pronounced thickening of sutures of apical plates should be briefly discussed. All species of Amphidomataceae share a distinct rim around the pore plate (with strains of *Az. spinosum* ribotype B as a notable exception; Tillmann et al., 2021), formed by thickened sutures of apical plates towards the pore plate. However, the pronounced thickening of the sutures between the lateral and dorsal apical plates, as observed in *Az. fusiforme*, distinguishes this species from most other *Azadinium* species, as this feature is otherwise only known from *Az. asperum* (Tillmann, 2018), both varieties of *Az. caudatum* (Nézan et al., 2012), and *Az. cuneatum* (Tillmann et al., 2014). In species that possess only very short sutures between the lateral and dorsal apical plates (such as *Az. concinnum*, *Az. polongum*, *Az. luciferelloides*, *Az. trinitatum*, and *Az. galwayense*), it is, however, difficult to discern and assess whether such sutures are thickened or not. Interestingly, suture thickenings of apical plates are present in all *Amphidoma* species examined so far by electron microscopy (*Am. languida* Tillmann, R. Salas & Elbrächter, *Am. parvula* Tillmann & Gottschling, *Am. trioculata* Tillmann, *Am. alata* Tillmann, *Am. cyclops* Tillmann, *Am. fulgens*, and *Am. pontica* Tillmann & Dzhembekova), although in *Am. languida*, *Am. fulgens*, and *Am. pontica*, the thickenings are usually restricted to some of these sutures, and in *Am. parvula*, they are only very weakly developed (Kuwata et al., 2024a, 2024b; Tillmann, 2018; Tillmann et al., 2012a, 2018, 2025). It therefore remains somewhat uncertain whether such suture thickenings reflect fundamental differences between *Amphidoma* and *Azadinium*. Notably, in all *Amphidoma* species studied in detail to date, the thickenings of the sutures of the lateral apical plates continue ventrally along the sutures with the distalmost precingular plates, whereas in all *Azadinium* species studied so far, these sutures are never thickened.

Azadinium fusiforme is phylogenetically placed within a clade comprising taxa that all share the morphological characteristic of possessing a ventral pore (vp) on the left side of plate 1', either at the anterior end or near the suture to plate 1" (Kuwata et al., 2023). Among these, however, all species with a vp positioned near the suture to plate 1"—namely *Az. fusiforme*, *Az. obesum*, *Az. spinosum*, and *Az.* cf. *spinosum*—are not closely related within the clade, suggesting that this trait may have evolved independently in several lineages.

The discovery of *Az. fusiforme* expands the known diversity of Amphidomataceae in the Pacific region and adds to the recent findings of Kuwata et al. (2025), which indicate that members of Amphidomataceae are more widely distributed in the Northwest Pacific than previously recognized. This lineage likely represents a persistent but previously overlooked component of the regional phytoplankton community, owing to its small cell size and generally low abundance. Metabarcoding studies based on environmental DNA (eDNA) have proven valuable for estimating the biogeographical distribution of *Azadinium* species. However, the partial SSU rDNA sequence of *Az. fusiforme* cannot be reliably distinguished from several congeners—specifically *Az. anteroporum*, *Az. dalianense*, *Az. galwayense*, *Az. poporum*, *Az. spinosum*, and *Az. trinitatum* in the V4 region, and *Az. anteroporum*, *Az. dalianense*, *Az. obesum*, *Az. poporum*, and *Az. trinitatum* in the V8–9 regions—indicating that molecular differentiation among *Azadinium* species remains challenging.

No known azaspiracids were detected in Korean strains (this study) or in the Japanese strain (Kuwata et al., 2025) of *Az. fusiforme*, and the untargeted screening for common AZA fragments (Sandvik et al., 2021) did not yield any identifiable peaks (this study). However, the close phylogenetic relationship of *Az. fusiforme* to *Az. poporum*—including the Korean lineage later shown to produce novel AZA-like analogues (Krock et al., 2012, 2015)—highlights the biochemical potential for structural diversification within the genus. Given the recurring occurrence of *Azadinium* species in Korean, Japanese, and Chinese coastal waters and their implications for shellfish safety, incorporating *Az. fusiforme* into regional harmful algal bloom surveillance and molecular monitoring programs will be crucial for advancing our understanding of the ecology, distribution, and toxic potential of Amphidomataceae in the Northwest Pacific.

CRediT authorship contribution statement

Urban Tillmann: Writing – review & editing, Writing – original draft, Investigation, Conceptualization. **Koyo Kuwata:** Writing – review & editing, Investigation. **Kyoungwon Cho:** Writing – review & editing, Investigation. **Kazuya Takahashi:** Writing – review & editing, Investigation. **Jan Tebben:** Writing – review & editing, Investigation. **Bernd Krock:** Writing – review & editing, Investigation. **Mitsunori Iwataki:** Writing – review & editing, Investigation, Conceptualization. **Sunju Kim:** Writing – review & editing, Writing – original draft, Investigation, Conceptualization.

Funding

This research was supported by grants from the National Research Foundation of Korea (RS-2024-00351443 and 2022M316A1085991) to SK, from the Korea Institute of Marine Science & Technology (KIMST) funded by the Ministry of Oceans and Fisheries (RS-2023-00256330) to SK, and from the Japan Society for the Promotion of Science (JSPS) KAKENHI (23K23681, 23KK0117) to MI, and (24KJ0853) to KK.

Acknowledgments

We greatly acknowledge technical support from Anne Müller and Thomas Max.

Appendix A. Supplementary data

Supplementary data to this article can be found online at https://doi.org/10.1016/j.ejop.2026.126182.

Data availability

Data will be made available on request.

References

Daugbjerg, N., Hansen, G., Larsen, J., Moestrup, Ø., 2000. Phylogeny of some of the major genera of dinoflagellates based on ultrastructure and partial LSU rDNA data, including the erection of three new genera of unarmoured dinoflagellates. Phycologia 39, 302–317.

Gu, H., Luo, Z., Krock, B., Witt, M., Tillmann, U., 2013. Morphology, phylogeny and azaspiracid profile of *Azadinium poporum* (Dinophyceae) from the China Sea. Harmful Algae 21–22, 64–75.

Guillard, R.R.L., Ryther, J.H., 1962. Studies on marine planktonic diatoms. I. *Cyclotella nana* Hustedt and *Detonula confervaceae* (Cleve) Gran. Can. J. Microbiol. 8, 229–239.

Handy, S.M., Bachvaroff, T.R., Timme, R.E., Coats, W.D., Kim, S., Delwiche, C.F., 2009. Phylogeny of four dinophysiacean genera (Dinophyceae, Dinophysiales) based on rDNA sequences from environmental samples. J. Phycol. 45, 1163–1174.

Katoh, K., Rozewicki, J., Yamada, K.D., 2019. MAFFT online service: multiple sequence alignment, interactive sequence choice and visualization. Brief. Bioinform. 20, 1160–1166.

Kim, S., Park, M.G., 2014. *Amoebophrya* spp. from the bloom-forming dinoflagellate *Cochlodinium polykrikoides*: parasites not nested in the "*Amoebophrya ceratii* complex". J. Eukaryot. Microbiol. 61, 173–181.

Krock, B., Tillmann, U., Voß, D., Koch, B.P., Salas, R., Witt, M., Potvin, E., Jeong, H.J., 2012. New azaspiracids in Amphidomataceae (Dinophyceae). Toxicon 60, 830–839.

Krock, B., Tillmann, U., Potvin, E., Jeong, H.J., Drebing, W., Kilcoyne, J., Al-Jorani, A., Twiner, M.J., Göthel, Q., Köck, M., 2015. Structure elucidation and in vitro toxicity of new azaspiracids isolated from the marine dinoflagellate *Azadinium poporum*. Mar. Drugs 13, 6687–6702.

Kuwata, K., Lum, W.M., Takahashi, K., Benico, G., Uchida, H., Ozawa, M., Matsushima, R., Watanabe, R., Oikawa, H., Suzuki, T., Iwataki, M., 2023. A new small thecate dinoflagellate *Azadinium anteroporum* sp. nov. (Amphidomataceae, Dinophyceae) isolated from the Asian Pacific. Phycologia 62, 303–314.

Kuwata, K., Hernández-Becerril, D.U., Ozawa, M., Uchida, H., Lum, W.M., Takahashi, K., Benico, G., Suzuki, T., Iwataki, M., 2024a. First report of toxigenic *Amphidoma languida* (Amphidomataceae, Dinophyceae) from the Pacific, with reference to intracellular ultrastructure and azaspiracid compounds. Phycol. Res. 72, 266–278.

Kuwata, K., Lum, W.M., Takahashi, K., Benico, G., Takahashi, K., Lim, P.T., Leaw, C.P., Uchida, H., Ozawa, M., Matsushima, R., Watanabe, R., Suzuki, T., Iwataki, M., 2024b. Phylogeny and ultrastructure of a non-toxigenic dinoflagellate *Amphidoma*

fulgens sp. nov. (Amphidomataceae, Dinophyceae), with a wide distribution across Asian Pacific. Harmful Algae 138, 102701.
Kuwata, K., Lum, W.M., Takahashi, K., Benico, G., Ozawa, M., Uchida, H., Numano, S., Watanabe, R., Matsushima, R., Suzuki, K., Iwataki, M., 2025. Diversity of amphidomatacean dinoflagellates in Japan, with a description of *Azadinium inconspicuum* sp. nov. and azaspiracid components in *Azadinium poporum* ribotypes. Harmful Algae 150, 102969.
Lundholm, N.; Bernard, C.; Churro, C.; Escalera, L.; Hoppenrath, M.; Iwataki, M.; Larsen, J.; Mertens, K.; Murray, S.; Probert, I.; Salas, R.; Tillmann, U.; Zingone, A. (Eds) (2009 onwards). IOC-UNESCO Taxonomic Reference List of Harmful Microalgae. Accessed at https://www.marinespecies.org/hab on 2025-11-20. doi:10.14284/362.
Luo, Z., Gu, H., Krock, B., Tillmann, U., 2013. *Azadinium dalianense*, a new dinoflagellate from the Yellow Sea, China. Phycologia 52, 625–636.
Luo, Z., Krock, B., Mertens, K., Nézan, E., Chomérat, N., Bilien, G., Tillmann, U., Gu, H., 2017. Adding new pieces to the *Azadinium* (Dinophyceae) diversity and biogeography puzzle: non-toxigenic *Azadinium zhuanum* sp. nov. from China, toxigenic *A. poporum* from the Mediterranean, and a non-toxigenic *A. dalianense* from the French Atlantic. Harmful Algae 66, 65–78.
Medlin, L., Elwood, H.J., Stickel, S., Sogin, M.L., 1988. The characterization of enzymatically amplified eukaryotic 16S-like rRNA-coding regions. Gene 71, 491–499.
Minh, B.Q., Schmidt, H.A., Chernomor, O., Schrempf, D., Woodhams, M.D., von Haeseler, A., Lanfear, R., 2020. IQ-TREE 2: new models and efficient methods for phylogenetic inference in the genomic era. Mol. Biol. Evol. 37, 1530–1534.
Nézan, E., Tillmann, U., Bilien, G., Boulben, S., Chèze, K., Zentz, F., Salas, R., Chomérat, N., 2012. Taxonomic revision of the dinoflagellate *Amphidoma caudata*: transfer to the genus *Azadinium* (Dinophyceae) and proposal of two varieties, based on morphological and molecular phylogenetic analyses. J. Phycol. 48, 925–939.
Nunn, G.B., Theisen, B.F., Christensen, B., Arctander, P., 1996. Simplicity-correlated size growth of the nuclear 28S ribosomal RNA D3 expansion segment in the crustacean order Isopoda. J. Mol. Evol. 42, 211–223.
Ozawa, M., Uchida, H., Watanabe, R., Matsushima, R., Oikawa, H., Takahashi, K., Iwataki, M., Suzuki, T., 2021. Complex profiles of azaspiracid analogues in two culture strains of *Azadinium poporum* (Amphidomataceae, Dinophyceae) isolated from Japanese coastal waters determined by LC-MS/MS. Toxicon 199, 145–155.
Ozawa, M., Uchida, H., Watanabe, R., Matsuchima, R., Oikawa, H., Takahashi, K., Iwataki, M., Suzuki, T., 2023. Azaspiracid accumulation in Japanese coastal bivalves and ascidians fed with *Azadinium poporum* producing azaspiracid-2 as the dominant toxin component. Toxicon 226, 107069.
Ozawa, M., Uchida, H., Numano, S., Watanabe, R., Matsushima, R., Oikawa, H., Takahashi, K., Iwataki, M., Suzuki, K., 2025. New azaspiracid analogues produced by *Azadinium spinosum* isolated from Japanese coastal waters. In: Proceedings of 20th International Conference on Harmful Algae, pp. 89–92.
Percopo, I., Siano, R., Rossi, R., Soprano, V., Sarno, D., Zingone, A., 2013. A new potentially toxic *Azadinium* species (Dinophyceae) from the Mediterranean Sea, *A. dexteroporum* sp. nov. J. Phycol. 49, 950–966.
Posada, D., 2008. ModelTest: Phylogenetic model averaging. Mol. Biol. Evol. 25, 1253–1256.
Potvin, E., Jeong, H.J., Kang, N.S.T., Tillmann, U., Krock, B., 2012. First report of the photosynthetic dinoflagellate genus *Azadinium* in the Pacific Ocean: morphology and molecular characterization of *Azadinium* cf. *poporum*. J. Eukaryot. Microbiol. 59, 145–156.
Rambaut, A., Drummond, A.J., Xie, D., Baele, G., Suchard, M.A., 2018. Posterior summarisation in Bayesian phylogenetics using Tracer 1.7. Syst. Biol. 67, 901–904.
Ronquist, F., Teslenko, M., van der Mark, P., Ayres, D.L., Darling, A., Höhna, S., Larget, B., Liu, L., Suchard, M.A., Huelsenbeck, J.P., 2012. MrBayes 3.2: efficient Bayesian phylogenetic inference and model choice across a large model space. Syst. Biol. 61, 539–542.
Sakamoto, S., Lim, W.A., Lu, D., Dai, X., Orlova, T., Iwataki, M., 2021. Harmful algal blooms and associated fisheries damage in East Asia: current status and trends in China, Japan, Korea and Russia. Harmful Algae 102, 101787.
Salas, R., Tillmann, U., Gu, H., Wietkamp, S., Krock, B., Clarke, D., 2021. Morphological and molecular characterization of multiple new *Azadinium* strains revealed a high diversity of non-toxigenic species of Amphidomataceae (Dinophyceae) including two new *Azadinium* species in Irish waters, North East Atlantic. Phycol. Res. 69, 88–115.
Sandvik, M., Miles, C.O., Lovberg, K.E., Kryuchkov, F., Wright, E.J., Mudge, E.M., Kilcoyne, J., Samdahl, I., 2021. In vitro metabolism of azaspiracids 1−3 with a hepatopancreatic fraction from blue mussels (*Mytilus edulis*). J. Agric. Food Chem. 69, 11322–11335.
Takahashi, K., Lum, W.M., Benico, G., Uchida, H., Ozawa, M., Oikawa, H., Suzuki, T., Nguyen, N.V., Ha, D.V., Iwataki, M., 2021. Toxigenic strains of *Azadinium poporum* (Amphidomataceae, Dinophyceae) from Japan and Vietnam, with first reports of *A. poporum* (ribotype A) and *A. trinitatum* in Asian Pacific. Phycol. Res. 69, 175–187.
Tamura, K., Stecher, G., Kumar, S., 2021. MEGA11: molecular evolutionary genetics analysis version 11. Mol. Biol. Evol. 38, 3022–3027.
Tillmann, U., 2018. Electron microscopy of a 1991 spring plankton sample from the Argentinean shelf reveals the presence of four new species of Amphidomataceae (Dinophyceae). Phycol. Res. 66, 269–290.
Tillmann, U., Akselman, R., 2016. Revisiting the 1991 algal bloom in shelf waters off Argentina: *Azadinium luciferelloides* sp. nov. (Amphidomataceae, Dinophyceae) as the causative species in a diverse community of other amphidomataceans. Phycol. Res. 64, 160–175.
Tillmann, U., Elbrächter, M., 2013. Cell division in *Azadinium spinosum* (Dinophyceae). Bot. Mar. 56, 399–408.
Tillmann, U., Elbrächter, M., Krock, B., John, U., Cembella, A., 2009. *Azadinium spinosum* gen. et sp. nov. (Dinophyceae) identified as a primary producer of azaspiracid toxins. Eur. J. Phycol. 44, 63–79.
Tillmann, U., Elbrächter, M., John, U., Krock, B., Cembella, A., 2010. *Azadinium obesum* (Dinophyceae), a new nontoxic species in the genus that can produce azaspiracid toxins. Phycologia 49, 169–182.
Tillmann, U., Elbrächter, M., John, U., Krock, B., 2011. A new non-toxic species in the dinoflagellate genus *Azadinium*: *A. poporum* sp. nov. Eur. J. Phycol. 46, 74–87.
Tillmann, U., Salas, R., Gottschling, M., Krock, B., O'Driscoll, D., Elbrächter, M., 2012a. *Amphidoma languida* sp. nov. (Dinophyceae) reveals a close relationship between *Amphidoma* and *Azadinium*. Protist 163, 701–719.
Tillmann, U., Söhner, S., Nézan, E., Krock, B., 2012b. First record of *Azadinium* from the Shetland Islands including the description of *A. polongum* sp. nov. Harmful Algae 20, 142–155.
Tillmann, U., Gottschling, M., Nézan, E., Krock, B., Bilien, G., 2014. Morphological and molecular characterization of three new *Azadinium* species (Amphidomataceae, Dinophyceae) from the Irminger Sea. Protist 165, 417–444.
Tillmann, U., Gottschling, M., Guinder, V., Krock, B., 2018. *Amphidoma parvula* (Amphidomataceae), a new planktonic dinophyte from the Argentine Sea. Eur. J. Phycol. 53, 14–28.
Tillmann, U., Wietkamp, S., Krock, B., Tillmann, A., Voss, D., Gu, H., 2020. Amphidomataceae (Dinophyceae) in the western Greenland area, including the description of *Azadinium perforatum* sp. nov. Phycologia 59, 63–88.
Tillmann, U., Wietkamp, S., Gu, H., Krock, B., Salas, R., Clarke, D., 2021. Multiple strains of *Azadinium spinosum* reveal diverse but stable toxin profiles, and a new nontoxigenic *Az.* cf. *spinosum*. Microorganisms 9, 134.
Tillmann, U., Dzhembekova, N., Vlas, O., Krock, B., Boicenco, L., Dursun, F., 2025. Diversity of Amphidomataceae (Dinophyceae) in the Black Sea, including description of *Amphidoma pontica* sp. nov. Phycol. Res. 73, 225–248.
Wong, T.K., Ly-Trong, N., Ren, H., Baños, H., Roger, A.J., Susko, E., Minh, B.Q., 2025. IQ-TREE 3: Phylogenomic Inference Software Using Complex Evolutionary Models.